KOPIO

DRAFT Technical Note #071

Not quite everything you always wanted to know about photon inefficiency

Laurence Littenberg

Physics Department
Brookhaven National Laboratory
Upton, N.Y. 11973 USA

15 Dec 2003

1. Introduction

In this note, I attempt to make sense of the available data and calculations on photon inefficiency, particularly for lead-scintillator sandwich counters. Some of the work on CsI is also relevant, as will be seen below. There are at least six contributions to photon inefficiency in sandwich counters: (1) photodetector/electronics noise, (2) backscattering, (3) leakage/punchthrough, (4) sampling fluctuations, (5) cracks, and (6) photonuclear interactions. Contribution (1) can readily be measured. Contributions (2)-(5) can be calculated with EGS or GEANT, (6) cannot, so it is the most problematic.

2. Photon inefficiency measurements

There are basically two sources of data on photon inefficiency in the region we are interested in. These are E787 and the series of experiments done in tagged photon beams in Japan.

2.1. E787 Results

E787 measured photon inefficiency by using $K^+ \to \pi^+\pi^0$ (henceforth $K\pi2$) events in which the π^+ and one of the γ's from the π^0 were detected, and the other γ probed. There were two studies, the first using the original E787 detector[1] and the second using the detector as it was configured after the 1992-4 upgrade[2]. Both studies attempted to "x-ray" the E787 detector using these gammas, which extended from 20 MeV to 222.5 MeV. I will use only the later, Sasaki[2], results. For the most part, I'll be dealing with the case in which the γ was aimed directly at the middle of the barrel veto, *i.e.* the bin that covered angles in the range $-0.2 < cos\theta_\gamma < 0.2$ (in the E787 coordinate system, $\theta = 0$ pointed down the beamline). Fig. 2.1 and Table 2.1 show these results in 20 MeV energy bins.

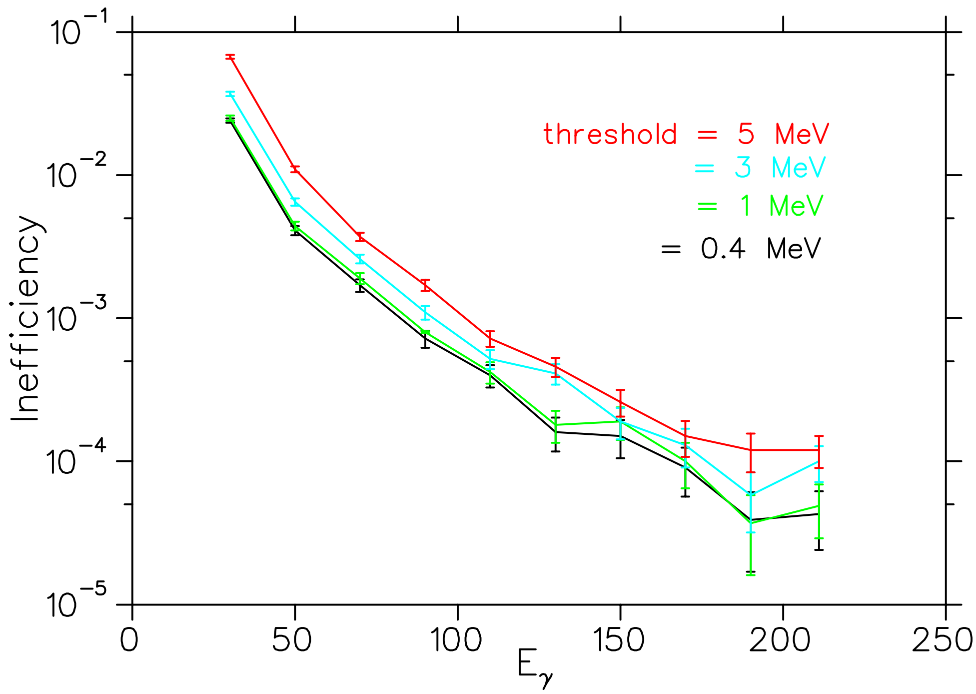

Figure 2.1: E787 photon inefficiency vs energy (from Sasaki[2]) for various thresholds: 5, 3, 1, and 0.4 MeV. Aside from a couple of statistical fluctuations, the lower the threshold, the lower the inefficiency. For $0.2 < cos\theta_\gamma < 0.2$.

Table 2.1: E787 photon inefficiency in units of 10^{-4} vs incident energy (from Sasaki[2]) for various thresholds. Thresholds are in terms of visible energy. For the $-0.2 < cos\theta_\gamma < 0.2$ bin.

E(MeV) \ Thresh	0.4MeV	1.0MeV	3.0MeV	5.0MeV
$20 - 40$	240 ± 9	250 ± 11	370 ± 13	670 ± 20
$40 - 60$	41 ± 3	44 ± 3.1	65 ± 3.7	110 ± 5
$60 - 80$	17 ± 1.7	19 ± 1.7	26 ± 1.9	37 ± 2.5
$80 - 100$	7.2 ± 1.0	8.0 ± 0.11	11 ± 1.2	17 ± 1.5
$100 - 120$	4.0 ± 0.71	4.2 ± 0.71	5.2 ± 0.77	7.2 ± 0.90
$120 - 140$	1.6 ± 0.43	1.8 ± 0.45	4.1 ± 0.66	4.6 ± 0.70
$140 - 160$	1.5 ± 0.45	1.9 ± 0.49	1.9 ± 0.47	2.6 ± 0.55
$160 - 180$	0.91 ± 0.34	1.0 ± 0.35	1.3 ± 0.39	1.5 ± 0.42
$180 - 200$	0.39 ± 0.22	0.37 ± 0.21	0.58 ± 0.26	1.2 ± 0.36
$200 - 222.5$	0.43 ± 0.19	0.49 ± 0.20	1.0 ± 0.28	1.2 ± 0.3

I will also comment on the results from the next nearest angle bins, those with $-0.5 < cos\theta_\gamma < -0.2$ and $0.2 < cos\theta_\gamma < 0.5$ Because the E787 is pretty nearly symmetric out to $|cos\theta_\gamma = .5|$, to get better statistics I average the results of these bins in Table 2.2.

Table 2.2: E787 photon inefficiency in units of 10^{-4} vs incident energy (from Sasaki[2]) for various thresholds. Thresholds are in terms of visible energy. Note that $E_{visible} \approx 0.3E_{deposited}$. I have averaged the $-0.5 < cos\theta_\gamma < -0.2$ and $0.2 < cos\theta_\gamma < 0.5$ bins.

E(MeV) \ Thresh	0.4MeV	1.0MeV	3.0MeV	5.0MeV
$20-40$	253 ± 7.9	273 ± 8	396 ± 11	670 ± 17
$40-60$	48 ± 2.6	51 ± 2.6	79 ± 3.4	120 ± 4.1
$60-80$	19 ± 1.5	19 ± 1.4	27 ± 1.6	39 ± 2.0
$80-100$	8.4 ± 0.92	9.1 ± 0.92	12 ± 1.0	17 ± 1.2
$100-120$	4.2 ± 0.62	4.3 ± 0.60	5.2 ± 0.64	7.2 ± 0.78
$120-140$	1.7 ± 0.38	1.8 ± 0.38	2.6 ± 0.46	3.9 ± 0.54
$140-160$	1.0 ± 0.30	1.0 ± 0.29	1.5 ± 0.34	1.9 ± 0.38
$160-180$	1.1 ± 0.32	0.99 ± 0.31	1.6 ± 0.36	1.8 ± 0.40
$180-200$	0.38 ± 0.21	0.39 ± 0.20	0.37 ± 0.19	0.73 ± 0.27
$200-222.5$	0.28 ± 0.16	0.57 ± 0.22	1.34 ± 0.32	1.62 ± 0.35

2.2. INS tagged photon beam studies - 1 (ES-147)

There were at least two such experiments at the INS electron synchrotron, but only the first, ES-147, seems to have been written up for publication[3]. The later experiment, ES-171 is the source of the data for a number of masters theses and reports, but no formal publications thus far. There was also a test using much higher energy photons from the LEPS backscattered laser beam at SPring-8. These tests focussed solely on measuring the photonuclear component of the photon inefficiency, since (1) it seemed possible to use their technique to probe it to very low levels, and (2) the remainder of the inefficiency should be reliably calculable via EGS. The technique was to surround a test counter, CsI or Pb/scint sandwich, with (12) neutron counters and to measure the response of the test counter when the photon tag signal plus at least one neutron was required†. Of course they couldn't detect all the neutrons, but they found that the occupation of the counters followed a Poisson distribution, allowing them to correct for the missed ones. This logic works if the neutrons all come from evaporation. If there are a lot of events with fast neutrons going forward (where there were no neutron counters) and no slow neutrons in the event, this would confound this method. For that reason, strictly speaking, the method gives a lower

† In some cases two neutron counters were required to fire.

limit to the photonuclear part of the inefficiency. A number of consistency checks were made, such as moving the test counter downstream with respect to the neutron counters, and these resulted in no evidence of a non-statistical contribution, which they interpreted as evidence that any corrections weren't too large. However there's been something of an evolution in the analysis of these experiments, suggesting that the systematics might not be completely under control. In ES-147, two configurations were tested. One was an array of 10 CsI counters, 30-cm thick ($\sim 16\ X_0$). The profile of this array was circular with about a 15cm diameter. The second configuration was a single Pb/scint sandwich counter with a 2mm Pb/6mm scintillator structure repeated 41 times ($\sim 15\ X_0$). This counter was hexagonal in cross section with a dimension of ~ 16 cm.

We are mainly interested in the results of the latter configuration, some of which are shown in Fig. 2.2 and Table 2.3.

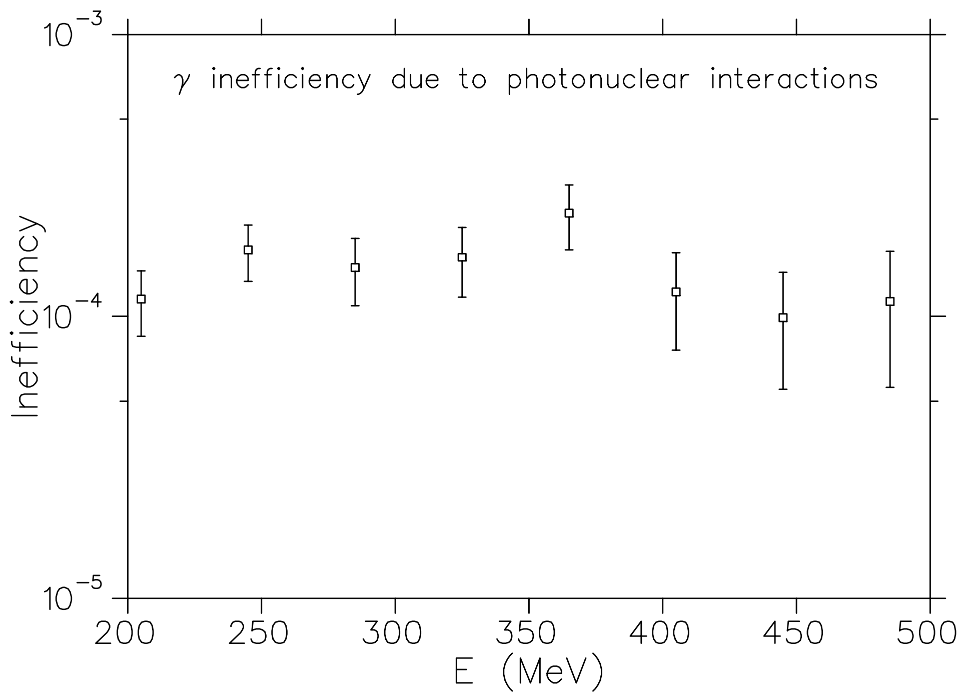

Figure 2.2: Photon inefficiency due to photonuclear interactions versus energy for a sandwich counter with 2mm Pb/6mm scint - from ES-147[3]. The threshold was 1 MeV in total energy, which corresponds to about 0.25MeV visible in the scintillator

Note that where the energy ranges of ES-147 and E787 overlap, the inefficiency due to photonuclear interactions measured by ES-147 is *larger* than what is measured by E787 for the *total* inefficiency. As we will see later, this is probably because of the thicker lead plates used in the shower counter of the Japanese experiment (2mm vs 1mm). The second column of Table 2.3 is the sum of contributions of the electromagnetic cascade (Contributions 2-4 of Section 1) to the inefficiency. These were calculated by the experimenters using EGS. The third column contains the contribution of punchthrough alone, this time calculated by me, using the mass attenuation coefficients made available by NIST[4] and included as

Table 2.3: Photon inefficiency in a 2mm Pb/6mm scintillator sandwich counter due to various sources in ES-147. The threshold is in the photonuclear measurement is 1 MeV total energy deposit. The third column is my hand calculation of the punch-through component.

photon energy (MeV)	Inefficiency (photonuclear) ($\times 10^{-4}$)	Inefficiency (EM-cascade) ($\times 10^{-5}$)	Inefficiency (punchthrough) ($\times 10^{-5}$)
205	1.15 ± 0.30	4.7 ± 1.0	4.60
245	1.72 ± 0.39	3.5 ± 0.5	3.94
285	1.49 ± 0.40	2.5 ± 0.4	3.38
325	1.62 ± 0.45	2.1 ± 0.4	3.04
365	2.32 ± 0.60	2.0 ± 0.3	2.81
405	1.22 ± 0.46	2.0 ± 0.3	2.61
445	0.99 ± 0.44	2.1 ± 0.3	2.41
485	1.13 ± 0.57	2.3 ± 0.4	2.24

Appendix A of this note. It was also necessary to assume a chemical composition for the scintillator. For this I took the data from the Bicron catalog[5] for BC-400 (NE102) which gives 5.23×10^{22} H atoms and 4.74×10^{22} C atoms/cm^3. The same proportions hold for BC-408, and BC-412. Using atomic weights of 1.008 Amu and 12.011 Amu, respectively, and 1.66054×10^{-24}g/Amu gives 0.08754 and 0.94538 g of H and of C respectively per cm^3 of scintillator. Therefore in the ES-147 Pb/scint counter there were 93.07g of Pb, 2.15g of H, and 23.26g of C. The numbers in the punchthrough column range from equal to those in the second column to about 2.5 σ high. Note that if the lead plates were something like 20μ thicker than the 2mm quoted in the reference, and their calculation took account of the actual thickness, it would bring the two columns into statistical agreement. In any case it seems clear that the electromagnetic component is dominated by punchthrough throughout this energy range.

There were a number of other very interesting results from ES-147. In particular the photonuclear inefficiency of the CsI was measured to be about 10 times smaller than that of the Pb/scint at 205 MeV, decreasing to $\lesssim 50$ times smaller than that of the Pb/scint at 485 MeV. What is particularly relevant is the distribution in observed energy of photonuclear events in the two cases. For the CsI, shown on the right of Fig. 2.3, these distributions are smooth and can be well-fit by a linear function. At the lowest energy, 205 MeV, this function has a mildly negative slope from $E_{obs} = 0$†. This slope goes flat at the $E_\gamma = 245$ MeV setting, then gets increasingly positive. As shown on the left of Fig. 2.3 the Pb/scint distributions are completely different, featuring a pronounced peak at $E_{obs} = 0$ for all

† Doug Bryman pointed out that in this figure the CsI data is much less finely binned than the Pb/scint so that peaks near 0 in the former might be hidden. However finer binned CsI data is available from ES-171 and it shows no peaks near 0.

photon energies. This is interpreted as due to photonuclear interactions whose products are potentially observable, but which fail to emerge from the lead in which they occur. The distributions imply there is something to be gained from using lead thinner than 2mm.

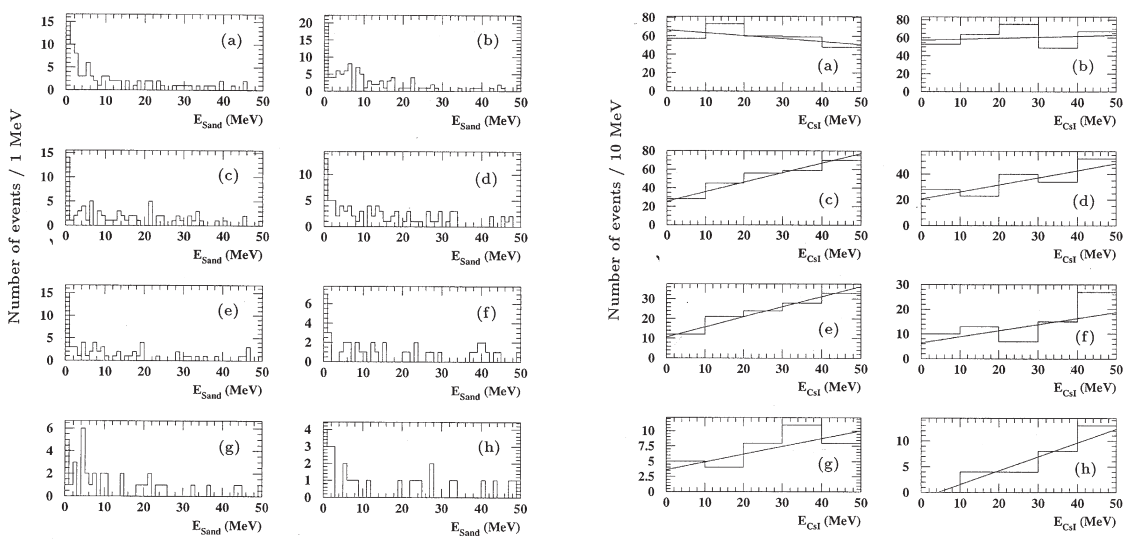

Figure 2.3: Observed energy in coincidence with apparent photonuclear events - from ES-147[3]. Left - Pb/scint, right - CsI. Graphs (a)-(h) are results from bins in average incident photon energy going from 205 to 485 MeV in 40 MeV intervals. In all cases the energy plotted is the total energy deposited in the counter.

Note there may have been some results from ES-147 not reported in Ajiumra *et al.*

2.3. INS tagged photon beam studies -2 (ES-171)

There seem to have been a number of measurements in this tagged beam made after ES-147. There are graphs in various talks and proposals that indicate this, and there are a number of Osaka and other university masters theses that report on them. Unfortunately most of the latter are in Japanese. As far as I can determine, all the subsequent tests done in the INS tagged photon beam were part of ES-171. The thesis of K. Mori[6] dealt with measurements on CsI, which is not our major concern, but some of the techniques used apparently first appeared there. One of the most interesting theses is that of Kurebayashi[7] which reports on measurements on Pb/scint sampling calorimeters of various types. In particular there were tests on 1mm Pb/5mm scintillator and on 0.5mm Pb/5mm scintillator counters. The former are particularly interesting because they correspond to the structure of the E787 barrel veto. Fig. 2.4 shows the inefficiency due to photonuclear interactions versus threshold, for both structures. The 0.5mm/5mm case was actually only 6.8 radiation lengths of such counters backed by by 18.4 radiation lengths of 1mm/5mm counters. It's notable, that above 200 MeV, where one can compare with Table 2.3, the inefficiencies shown here are considerably lower than those from the 2mm/6mm structure studied in

ES-147. It's hard to read off the graphs with any precision, but to take an example for a 1 MeV threshold, the E_γ=205 MeV result for 1mm/5mm is about 2.4×10^{-5} compared to $(11.5 \pm 3.0) \times 10^{-5}$ for 2mm/6mm. The 0.5mm/5mm result is even smaller, but the error bar is large. This is a general feature of the results, *i.e.* for low incident energy and for low threshold the the 0.5mm/5mm result is lower than that of 1mm/5mm, but it is hard to be sure because the error is rather large (the ratios of the photonuclear inefficiency of these two configuration are shown in Fig. C.2). These results support the idea that making the lead thinner can help fight the photonuclear effect. It's clear that 1mm is better than 2mm, but it's less clear how much benefit one can gain by going further. The data seems to support some continued improvement for $E_\gamma \lesssim 200$ MeV and $E_{thresh} \lesssim 5$ MeV.

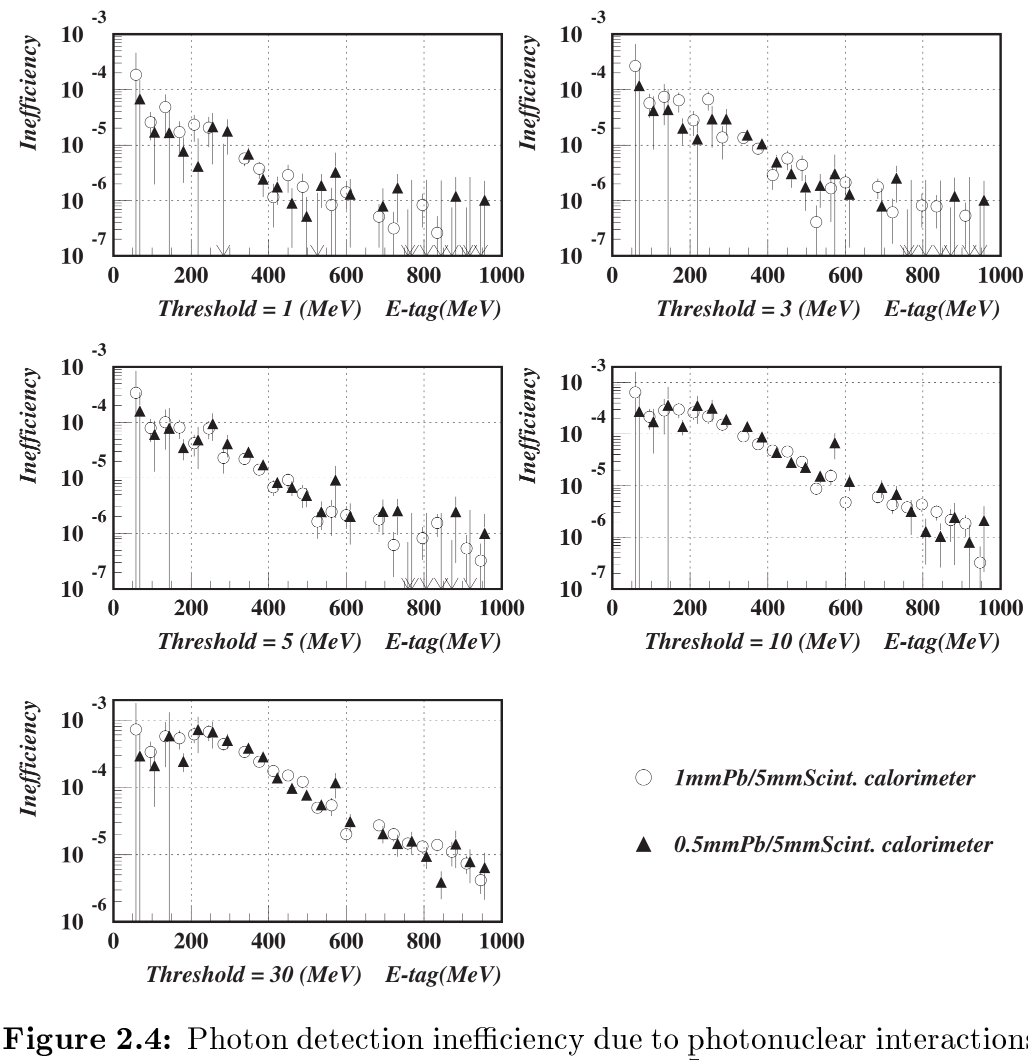

Figure 2.4: Photon detection inefficiency due to photonuclear interactions versus incident photon energy from Kurebayashi[7]. Results for both the Pb/scint=1mm/5mm and 0.5mm/5mm structures are shown, for several different thresholds. Note that 0.5mm/5mm case was actually 6.8 X_0 of that structure followed by 18.4 X_0 of the 1mm/5mm counters. I believe the thresholds are meant to be in terms of total energy deposited in the counter, **not** visible energy.

One should be able to put a bound on the possible improvement by comparing with the CsI results. In Table 2.4 I attempt to read off the values of on the upper left hand graph of Fig. 2.4 and compare them with results from ES-147. The result seems to show that most of the possible benefit is achieved by the 1mm/5mm structure, and that it really doesn't seem worth it to push beyond 0.5mm/5mm, at least as far as one can probe (one's knowledge is limited by the results on CsI). However one should note that the fact that in KOPIO the photons will often impinge on the vetoes at rather oblique angles argues for thinner plates.

Table 2.4: Photon inefficiency due to photonuclear interactions from ES-147 and the Kurebayashi thesis. Threshold is 1 MeV in total energy deposited.

photon energy (MeV)	Inefficiency CsI ($\times 10^{-5}$)	Inefficiency 2/6mm Pb/scint ($\times 10^{-5}$)	Inefficiency 1/5mm Pb/scint ($\times 10^{-5}$)	Inefficiency 0.5/5mm Pb/scint ($\times 10^{-5}$)
205	1.11 ± 0.15	11.5 ± 3.0	$2.35^{+1.07}_{-1.18}$	$0.40^{+0.87}_{-0.40}$
245	1.12 ± 0.15	17.2 ± 3.9	$2.05^{+1.11}_{-1.14}$	$2.15^{+1.63}_{-1.70}$
285	0.71 ± 0.13	14.9 ± 4.0	< 1.0	$1.77^{+1.04}_{-1.08}$
325	0.81 ± 0.15	16.2 ± 4.5	$0.57^{+0.15}_{-0.16}$	$0.70^{+0.19}_{-0.22}$
365	0.39 ± 0.11	23.2 ± 6.0	$0.37^{+0.14}_{-0.13}$	0.24 ± 0.13
405	0.37 ± 0.12	12.2 ± 4.6	$0.12^{+0.08}_{-0.09}$	$0.18^{+0.08}_{-0.09}$
445	0.21 ± 0.09	9.9 ± 4.4	$0.29^{+0.14}_{-0.15}$	0.09 ± 0.08
485	< 0.13	11.3 ± 5.7	$0.18^{+0.12}_{-0.13}$	$0.05^{+0.06}_{-0.05}$

Another report from ES-171 was the Saga masters thesis of H. Watanabe[8], in which there's data from a the test of a sandwich counter with 1mm/3mm Pb/scint structure in ES-171. Fig. 2.5, from this thesis, compares the photonuclear-induced inefficiency of this counter with that of the 2mm/6mm counter tested in ES-147. One sees graphically the big improvement obtained by going from 2mm to 1mm plates.

Watanabe later wrote an internal report[9](in English) which appears to refine the analysis of his thesis and that of Mori.

An exception to the use of Japanese for writing up ES-171 results is the thesis of T. Matsumura[10]. It gives results on a 50cm-long CsI counter and also Pb/scintillator sandwich counters of 1mm/3mm, 1mm/5mm, and 0.5mm/5mm structure. It unfortunately contains few details and results with a 10 MeV threshold only.

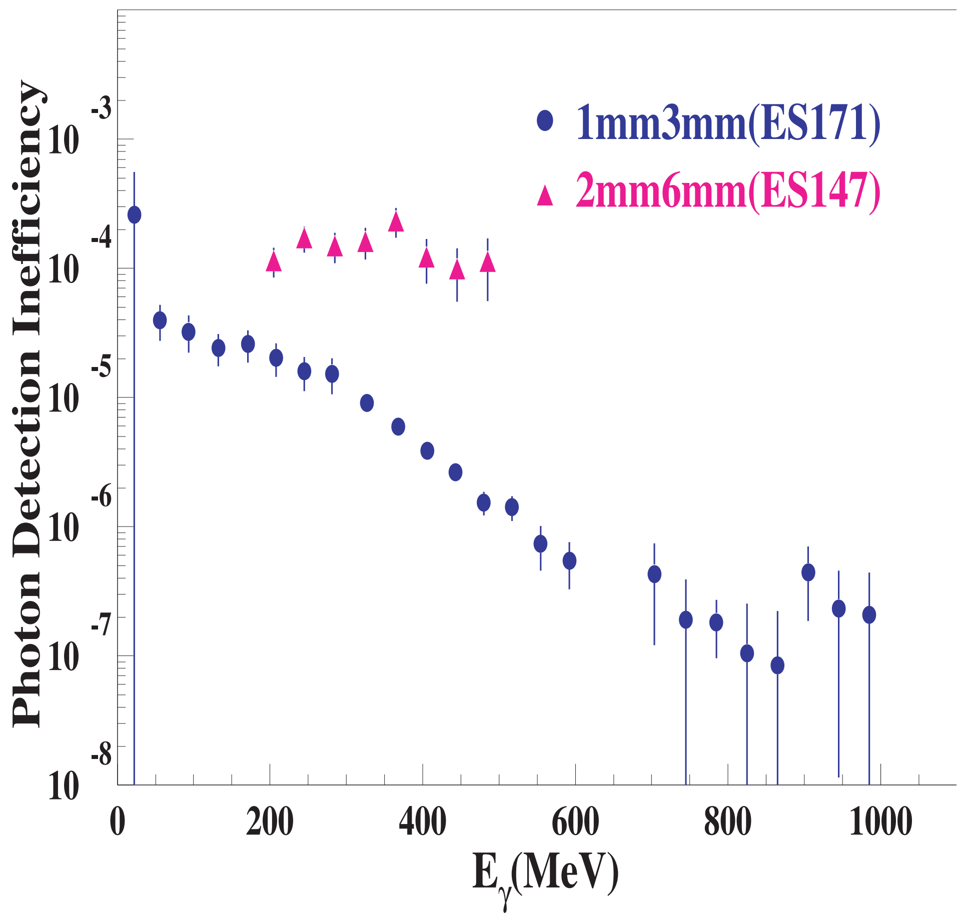

Figure 2.5: Photon detection inefficiency due to photonuclear interactions versus incident photon energy from H. Watanabe's thesis[8]. Results for Pb/scint=1mm/3mm and 2mm/6mm are shown. I believe the threshold is 1 MeV in total deposited energy.

2.4. SPring-8

Much of the apparatus used in ES-147 and ES-171 seems to have been taken to the SPring-8 light source and put into the LEPS tagged photon beam. However here, the photon energies used were much higher (~ 2 GeV). Other differences were the use of only 8 neutron counters (four on each side and none on top) and a different Pb/scint sandwich counter. This one was made of three 1mm/5mm modules, each with 16 layers, for a total of only 10.2 X_0. The transverse cross-section of each module was square with dimension 15 cm. Although the energy range is not relevant to KOPIO, one can learn something about the general techniques used in this series of experiments since there's a good thesis in English[11]. The experiment seemed to be statistics limited, so the whole 1.5-2.4 GeV range was treated together. The result for CsI was $(2.93 \pm 0.89^{+1.15}_{-0.44}) \times 10^{-7}$ where the first error was statistical and the second was systematic and the result for the lead-scintillator was $(8.3 \pm 1.7^{+13.5}_{-1.2}) \times 10^{-7}$.

3. Understanding the E787 measurements

There have been a number of previous attempts to understand the E787 photon inefficiency, but I'm not entirely happy with them. I describe a number of them below and then try to improve upon them.

3.1. Previous attempts

The E787 Monte Carlo, UMC, was perhaps unfortunately initiated just before GEANT became generally available. It does contain EGS, so should simulate purely electromagnetic interactions in the same way that GEANT 3 does. Dan Marlow inserted the PICA photonuclear code into UMC[12]. This code simulates the primary photonuclear interaction and high energy tertiaries. He later used it to help decide the detector geometry[13]. In 1986, Craig Woody did a similar exercise[14] directed toward possible upgrades. In 1989 Peter Meyers measured the π^0 inefficiency[15] in the course of a search for the process $\pi^0 \to \nu\bar{\nu}$. Still later Peter added code to UMC to deal with the evaporation energy down to 8 MeV (PNEVAP) and to handle neutron propagation and interaction. He used the upgraded version of UMC to simulate the photon inefficiency data available in 1990[16]. In 1992, Akira Konaka improved the neutron propagation of the program[17] and used it to determine weak areas for photon vetoing in the detector, so that these could be addressed in the upgrade in progress at the time. Later, Masahiro Kazumori did further simulations[18] in the course of working on the barrel veto liner upgrade, which was eventually completed as part of mounting E949.

The problem with these studies for the present purpose is that the results quoted tend to be integrated over the whole detector and over wide energy ranges (typically the full 20-222.5 MeV range of photon energy is divided in two). They agreed with the available data about as well as the known uncertainties allowed, but the kind of detailed comparisons that would allow a full understanding of the limits on efficiency were not made. It's clear that some very straightforward UMC studies would be very welcome. For example it would be useful to direct photons of various energies from the center of the stopping target at $-0.2 < cos\theta_\gamma < 0.2$ for comparison with the Sasaki data. Photonuclear reactions should be turned off so that we can assess the effects of sampling fluctuations and check my hand calculations of punchthrough.

Now although no one from E787 seems to have made the calculation I'd like, there are some relevant calculations in the Osaka masters thesis of K. Manabe[19]. This work attempted to use the results of the tagged beam measurements to assess possible approaches to a $K_L \to \pi^0\nu\bar{\nu}$ experiment. In order to characterize the total photon detection inefficiency, Manabe made an EGS simulation of one of the sandwich counters referred to in the Kurebayashi thesis, *i.e.* an 18.2 $X_0$1mm Pb/5mm scintillator. He also simulated an 18.8 X_0 0.5mm Pb/5mm scintillator system and an 18.3 X_0 0.1mm Pb/5mm scintillator system. Manabe's calculation of the Kurebayashi counter can be used to extract information on the sampling fluctuation contribution to the E787 results. In principle, his results also contain other useful information. Fig. 3.1 shows his distributions of visible energy resulting from incident photons of 20-100 MeV for the 1mm/5mm and 0.5mm/5mm cases. The shaded portion of the curves corresponds to a 10 MeV threshold in terms of the incident energy which is essentially the same as the **total** energy deposited in the counter. Manabe gives the following connection between the two quantities:

$$\begin{aligned} E_{vis} &= 0.3381E_{inc} - 0.1491\text{MeV} \\ E_{vis} &= 0.5141E_{inc} - 0.1309\text{MeV} \\ E_{vis} &= 0.8475E_{inc} - 0.1138\text{MeV} \end{aligned} \tag{3.1}$$

where the three lines in Eq. (3.1) refer to the 1mm/5mm, 0.5mm/5mm, and 0.1mm/5mm cases respectively. The top line should be compared with $E_{vis} \approx 0.3E_{inc}$ for E787.

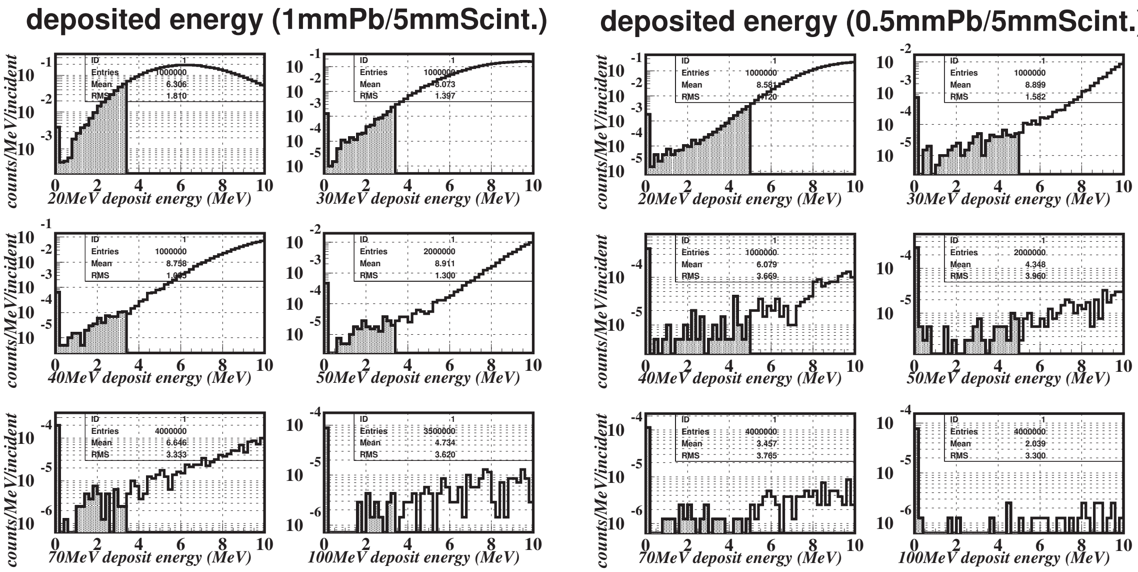

Figure 3.1: Manabe EGS calculations of sandwich counter responses to photons of various energies[19]. Left plots are for 96 layers of 1mm Pb/5mm scintillator. Right plots are for 187 layers of 0.5mm Pb/5mm scintillator. Abscissa of plots is visible energy, i.e. energy in scintillator in bins of 0.2 MeV. Shaded region corresponds to 10 MeV total energy deposited in the counter.

Fig. 3.1 is very instructive. The peaks near 0 are due to punchthrough and can be used to compare with my hand calculations. For example for E_{inc} = 50MeV and the 1mm/5mm case, the peak height is $\sim 5 \times 10^{-4}$. One must divide this by 5, because the ordinate of the graphs is counts/MeV and the bin widths are 0.2MeV. Thus the graph shows a punchthrough of $\sim 10^{-4}$. This is to be compared with my hand calculation of 0.76×10^{-4}. Similarly, the 100 MeV graph gives a punchthrough of $\sim 1.8 \times 10^{-5}$ and my hand calculation gives 1.93×10^{-5}. With this level of agreement, it's worth trying to use the graphs to get the contribution of sampling fluctuations†. Table 3.1 shows the result for the 1mm Pb/5mm scintillator structure. I have done the same exercise for the 0.5mm Pb/5mm scintillator and the 0.1mm Pb/5mm scintillator cases. The resulting tables can be found in Appendix B.

† I imported the figures into Adobe Illustrator and used the measuring facilities in that program to sum up the values in the graphs as best I could.

Table 3.1: Photon inefficiency in a 1mm Pb/5mm scintillator sandwich counter due to sampling fluctuations calculated by Manabe[19]. The thresholds are in terms of visible energy.

photon energy (MeV)	Inefficiency th 0.4 MeV ($\times 10^{-4}$)	Inefficiency th 1.0 MeV ($\times 10^{-4}$)	Inefficiency th 3.0 MeV ($\times 10^{-4}$)	Inefficiency th 5.0 MeV ($\times 10^{-4}$)
20	1.7	7.4	316	2450
30	0.038	0.37	8.77	15.5
40	0.024	0.08	0.90	7.34
50	0.015	0.04	0.38	1.16
70	0.007	0.015	0.082	0.23
100	0.005	0.01	0.03	0.074

3.2. My own attempt to understand the E787 results

As mentioned, we really need a custom EGS calculation to nail down the electromagnetic contributions, but since none is yet available I'll try to make do with what we have.

First, let's address photostatistics. There were about 10 p.e./visible MeV in the E787 barrel veto (BV). About 30% of the deposited energy is visible, so for 20 MeV, the lowest photon energy available from $K\pi 2$'s, one would have ~ 60 photo-electrons. If the threshold were 1 MeV of visible energy, one would be asking how likely it was for 60 p.e. to fluctuate down to 10. This is about a 7 σ excursion, so one doesn't expect a significant contribution.

Next, how about sampling fluctuations? We can try using Manabe's calculations in the form of the information of Table 3.1, at least up to 100 MeV. Another way to get an idea of the size of this contribution is from the observed resolution of the E787 BV, which is about $\sigma_E/E = 0.065/\sqrt{E}$. Thus, for example, for $E = 30$MeV, one has $E_{vis} = 9 \pm 3.38$MeV. This is 2.369σ from the threshold of 1 MeV, so should account for an inefficiency of 0.00893. Similar calculations for 60, 100, and 140 MeV give 1.86×10^{-4}, 1.28×10^{-6}, and 9.58×10^{-9} respectively. In general, assume $\sigma_E/E = \alpha/\sqrt{E}$, and $\epsilon = \beta E$, where ϵ is the visible energy (as mentioned above, in the case of E787, $\beta \approx 0.3$). Then $\sigma_\epsilon = \alpha\beta\sqrt{E}$. For a given threshold, $\epsilon = \eta$, one is simply asking how many σ_ϵ's away from the central value the threshold is. The answer is $(\beta E - \eta)/\alpha\beta\sqrt{E}$. The numerical value we are seeking is then given by

$$\begin{aligned} \xi &= \frac{1}{2}\left[1 - \mathrm{erf}\left(\frac{\beta E - \eta}{\alpha\beta\sqrt{2E}}\right)\right] \\ &= \frac{1}{2}\mathrm{erfc}\left(\frac{0.3E\,(GeV) - .001}{.02758\sqrt{E\,(GeV)}}\right) \end{aligned} \qquad (3.2)$$

Note that both methods will overestimate the sampling fluctuation contribution in E787 by up to a factor 2, since there's about 1 X_0 (46cm) of scintillator in front of the BV, so that half the photons convert before encountering any sampling calorimeter. However we'll ignore this effect for now since it is hard to estimate without a proper Monte Carlo. It's clear that this component is negligible for $E \gtrsim 100$MeV, as can be seen in Table 3.2 † Note that this procedure gives much larger results than are given by the Manabe calculations.

The next component to calculate is that of the punchthrough. For this, one needs to know that a photon at 90° in the E787 detector had to penetrate 6cm of scintillator in the stopping target, followed by 0.375" of I-counter scintillator, a low-mass drift chamber, and 15.375" of range stack scintillator, before entering the BV. The BV itself was 75 layers of 1mm Pb and 5mm scintillator[20]. Thus in total, one had 85.125g of Pb, and 83.505 cm of scintillator. Using the proportions given in Section 2.2, this corresponds to 7.31g of hydrogen and 78.94g of carbon. We must make a small correction due to the fact that the data includes tracks at a small inclination to the apparatus (*i.e.* $-0.2 < cos\theta_\gamma < 0.2$):

$$\int_{-.2}^{.2} \frac{1}{sin\theta_\gamma} dcos\theta_\gamma / \int_{-.2}^{.2} dcos\theta_\gamma = 1.00679. \tag{3.3}$$

Then, using the mass attenuation coefficients given in Appendix A yields the values in Table 3.2. Note that if we add the components at the highest energy in this table to the photonuclear result at 205 MeV from Table 2.4, we get a predicted inefficiency of $(0.65^{+0.11}_{-0.12}) \times 10^{-4}$, in reasonable agreement with the E787 measured value of $(0.43 \pm 0.19) \times 10^{-4}$ at 0.4 MeV threshold. Note that the "1 MeV" threshold for the photonuclear case corresponds to a 0.34 MeV threshold for E787.

Let's see if we can match some other E787 points. First, we need some Kurebayashi data that is not in Table 2.4. Table C.1 of Appendix C contains additional photonuclear results from Kurebayashi[7]. I drew a smooth curve through these points on a log scale and obtained photonuclear inefficiency values for the energies measured by E787. These are given in the sixth column of Table 3.2. Note the value for $E_\gamma = 211.25$ MeV comes out a little lower than in the estimate of the last paragraph since information from nearby points is added. Finally in the last column of Table 3.2, I add up the sampling, punchthrough and photonuclear components. The agreement with the E787 measurements is acceptable down to about 150 MeV, but then the data start to pull away. By 110 MeV, the data point is unmistakably higher than the sum of components. It's not possible to make the comparison below 70 MeV where the photonuclear results run out, but it seems that the lower energy points would require a huge rise in the photonuclear component to explain the discrepancy (i.e. it would need to rise from 1.17×10^{-4} at 70 MeV to $\sim 30 \times 10^{-4}$ at 50 MeV and to $\sim 80 \times 10^{-4}$ at 30 MeV).

It's instructive to do a similar exercise with the data from the $-0.5 < cos\theta_\gamma < -0.2$ and $0.2 < cos\theta_\gamma < 0.5$ bins, whose data is available in Table 2.2. Table 3.3 shows the results.

What's interesting here is that although one would expect that both the sampling fluctuation and the photonuclear components would get larger for the more inclined tracks, the observed inefficiency stays roughly the same, or even decreases. The one component that will clearly decrease is the punchthrough, which is evident in comparing Table 3.3

† This procedure tends to underestimate the effect, since there must non-Gaussian tails to the resolution at some level.

Table 3.2: Photon inefficiency due to various sources in E787, for $-0.2 < cos\theta_\gamma < 0.2$. In units of 10^{-4}. The second entry in the sampling fluctuation column comes from Manabe's calculation. Since the sampling fluctuation component changes rapidly through the 30 MeV bin (really 20-40 MeV), I averaged the 20, 30 and 40 MeV values for the sampling fluctuation component in that bin.

photon energy	Ineff. Th=0.4 MeV	Ineff. Th=1 MeV	Ineff. (smpl)	Ineff. (pnchth)	Ineff. (PN)	Ineff. sum
30 MeV	240 ± 9	250 ± 11	154/2.6	7.00	?	161+?
50	41 ± 3	44 ± 3.1	6.62/0.04	3.05	?	9.67+?
70	17 ± 1.7	19 ± 1.7	0.53/0.015	1.83	1.17	3.43
90	7.2 ± 1.0	8.0 ± 0.11	0.044	1.24	0.50	1.78
110	4.0 ± 0.71	4.2 ± 0.71	0.004	0.94	0.33	1.27
130	1.6 ± 0.43	1.8 ± 0.45	0.0003	0.78	0.26	1.04
150	1.5 ± 0.45	1.9 ± 0.49		0.61	0.22	0.83
170	0.91 ± 0.34	1.0 ± 0.35		0.53	0.21	0.74
190	0.39 ± 0.22	0.37 ± 0.21		0.47	0.19	0.66
211.25	0.43 ± 0.19	0.49 ± 0.20		0.41	0.18	0.57

Table 3.3: Photon inefficiency due to various sources in E787. For $-0.5 < cos\theta_\gamma < -0.2$ and $0.2 < cos\theta_\gamma < 0.5$ In units of 10^{-4}.

photon energy	Ineff. Th=0.4 MeV	Ineff. Th=1 MeV	Ineff. (smpl)	Ineff. (pnchth)	Ineff. (PN)	Ineff. sum
30 MeV	253 ± 7.9	273 ± 8	154/2.6	4.31	?	158+?
50	48 ± 2.6	51 ± 2.6	6.62/0.04	1.78	?	8.4+?
70	19 ± 1.5	19 ± 1.4	0.53/0.015	1.03	1.17	2.73
90	8.4 ± 0.92	9.1 ± 0.92	0.044	0.68	0.50	1.22
110	4.2 ± 0.62	4.3 ± 0.60	0.004	0.51	0.33	0.84
130	1.7 ± 0.38	1.8 ± 0.38	0.0003	0.41	0.26	0.67
150	1.0 ± 0.30	1.0 ± 0.29		0.32	0.22	0.54
170	1.1 ± 0.32	0.99 ± 0.31		0.27	0.21	0.48
190	0.38 ± 0.21	0.39 ± 0.20		0.24	0.19	0.43
211.25	0.28 ± 0.16	0.57 ± 0.22		0.21	0.18	0.39

with Table 3.2. This because the correction factor corresponding to that of Eq. (3.3) in this case is 1.0741 instead of 1.00679. This is further evidence that the punchthrough is a very important effect in the E787 data, at least for the higher energies.

Although it appears we understand the E787 results above ~ 150 MeV, below that energy, it is much more difficult to fathom.

4. Implications for KOPIO

Firstly, punchthrough might not be negligible for the BV, for certain energies. Marvin Blecher tells me our GEANT assumes 8 modules with 11 1mm Pb/7mm scintillator layers in. Thus a photon at normal incidence will encounter 8.8cm of lead and 61.6cm of scintillator. This comes to 99.88g of lead, 58.24 g of carbon and 5.39g of hydrogen. For 200 MeV photons, the punchthrough will be $e^{-11.18} = 1.39 \times 10^{-5}$. This is probably comparable to the photonuclear contribution, which, according to ES-171 is about 1.8×10^{-5} for a 1mm Pb/5mm scint structure and so would presumably be a little less for 1mm Pb/7mm scint. However since most photons are not at normal incidence, it's not clear how big a problem this will be – GEANT can certainly tell us. Around 200 MeV is probably the maximum for the effects of punchthrough. Much below that other effects seem to dominate (judging by the E787 results) and by 400 MeV, the punchthrough at normal incidence will be down to 7.3×10^{-6}.

Marvin did a GEANT calculation for the KOPIO BV for photons at normal incidence for a few energies. I include it in Table 4.1, along with my hand calculation of the punchthrough.

Table 4.1: Calculations of inefficiency due to electromagnic interactions for photons at normal incidence to the KOPIO BV. M. Blecher used a 5 MeV visible energy threshold. Punchthrough is my calculation.

photon energy (MeV)	Inefficiency MB GEANT ($\times 10^{-4}$)	Inefficiency punchthrough ($\times 10^{-4}$)
25	1000	13.0
50	6.0	3.18
100	0.5	0.33
150	0.2	0.18

5. Some tentative conclusions

First, it seems that to avoid photonuclear losses, lead-scintillator sandwich counters must have lead layers less than 2mm. For photons at normal incidence, most of the potential benefit seems to be obtained by 1mm plates, although there is statistically weak evidence indicating some improved benefit going to 0.5mm lead plates, particularly at low energies.

Second, it seems as if the E787 results at the highest energies can be explained in terms of the photonuclear measurements of ES-171 plus the calculated effects of punchthrough.

Third, it's actually possible that KOPIO could benefit from a thicker barrel than the one presently planned.

6. Questions evoked by this study

1. As far as photonuclear inefficiency is concerned, what is the difference between a plate of thickness t at normal incidence and a plate of thickness $t' < t$ at $cos\theta = t'/t$?
2. As far as sampling fluctuations are concerned, what is the difference between a plate of thickness t at normal incidence and a plate of thickness $t' < t$ at $cos\theta = t'/t$?
3. What is the true contribution of sampling fluctuations on the E787 photon detection inefficiency, particularly at low energies?
4. If sampling fluctuations can't explain it, what is the main contributor to the large low-energy photon detection inefficiency in E787?

Appendix A.
Mass attenuation coefficients

One can get the photon mass attenuation coefficients for elements, mixtures and compounds at http::/physics.nist.gov/PhysRefData/Xcom/Text/XCOM.html. Here are the ones for lead, in Fig. A.1 and Fig. A.2, for Carbon in Fig. A.3 and Fig. A.4, and for Hydrogen in Fig. A.5 and Fig. A.6.

XCOM:

Constituents (Atomic Number : Fraction by Weight)

Z=82 : 1.000000

	PHOTON ENERGY (MeV)	SCATTERING COHERENT (cm2/g)	SCATTERING INCOHER. (cm2/g)	PHOTO-ELECTRIC ABSORPTION (cm2/g)	PAIR PRODUCTION IN NUCLEAR FIELD (cm2/g)	PAIR PRODUCTION IN ELECTRON FIELD (cm2/g)	TOTAL ATTENUATION WITH COHERENT SCATT. (cm2/g)	TOTAL ATTENUATION WITHOUT COHERENT SCATT. (cm2/g)
	1.000E-03	1.25E+01	3.59E-03	5.20E+03	0.00E+00	0.00E+00	5.21E+03	5.20E+03
	1.500E-03	1.20E+01	6.60E-03	2.34E+03	0.00E+00	0.00E+00	2.36E+03	2.34E+03
	2.000E-03	1.14E+01	9.62E-03	1.27E+03	0.00E+00	0.00E+00	1.29E+03	1.27E+03
	2.484E-03	1.09E+01	1.24E-02	7.90E+02	0.00E+00	0.00E+00	8.01E+02	7.90E+02
82 M5	2.484E-03	1.09E+01	1.24E-02	1.38E+03	0.00E+00	0.00E+00	1.40E+03	1.38E+03
	2.534E-03	1.08E+01	1.27E-02	1.64E+03	0.00E+00	0.00E+00	1.65E+03	1.64E+03
	2.586E-03	1.08E+01	1.30E-02	1.93E+03	0.00E+00	0.00E+00	1.94E+03	1.93E+03
82 M4	2.586E-03	1.08E+01	1.30E-02	2.44E+03	0.00E+00	0.00E+00	2.45E+03	2.44E+03
	3.000E-03	1.03E+01	1.52E-02	1.95E+03	0.00E+00	0.00E+00	1.96E+03	1.95E+03
	3.066E-03	1.02E+01	1.56E-02	1.85E+03	0.00E+00	0.00E+00	1.86E+03	1.85E+03
82 M3	3.066E-03	1.02E+01	1.56E-02	2.14E+03	0.00E+00	0.00E+00	2.15E+03	2.14E+03
	3.301E-03	9.93E+00	1.68E-02	1.78E+03	0.00E+00	0.00E+00	1.79E+03	1.78E+03
	3.554E-03	9.65E+00	1.81E-02	1.49E+03	0.00E+00	0.00E+00	1.50E+03	1.49E+03
82 M2	3.554E-03	9.65E+00	1.81E-02	1.57E+03	0.00E+00	0.00E+00	1.58E+03	1.58E+03
	3.699E-03	9.50E+00	1.89E-02	1.43E+03	0.00E+00	0.00E+00	1.44E+03	1.43E+03
	3.851E-03	9.34E+00	1.96E-02	1.30E+03	0.00E+00	0.00E+00	1.31E+03	1.30E+03
82 M1	3.851E-03	9.34E+00	1.96E-02	1.36E+03	0.00E+00	0.00E+00	1.37E+03	1.36E+03
	4.000E-03	9.18E+00	2.04E-02	1.24E+03	0.00E+00	0.00E+00	1.25E+03	1.24E+03
	5.000E-03	8.21E+00	2.52E-02	7.22E+02	0.00E+00	0.00E+00	7.30E+02	7.22E+02
	6.000E-03	7.36E+00	2.97E-02	4.60E+02	0.00E+00	0.00E+00	4.67E+02	4.60E+02
	8.000E-03	6.00E+00	3.81E-02	2.23E+02	0.00E+00	0.00E+00	2.29E+02	2.23E+02
	1.000E-02	4.98E+00	4.54E-02	1.26E+02	0.00E+00	0.00E+00	1.31E+02	1.26E+02
	1.304E-02	3.85E+00	5.44E-02	6.31E+01	0.00E+00	0.00E+00	6.70E+01	6.32E+01
82 L3	1.304E-02	3.85E+00	5.44E-02	1.58E+02	0.00E+00	0.00E+00	1.62E+02	1.58E+02
	1.500E-02	3.31E+00	5.92E-02	1.08E+02	0.00E+00	0.00E+00	1.12E+02	1.08E+02
	1.520E-02	3.26E+00	5.96E-02	1.04E+02	0.00E+00	0.00E+00	1.08E+02	1.05E+02
82 L2	1.520E-02	3.26E+00	5.96E-02	1.45E+02	0.00E+00	0.00E+00	1.49E+02	1.45E+02
	1.553E-02	3.18E+00	6.04E-02	1.38E+02	0.00E+00	0.00E+00	1.41E+02	1.38E+02
	1.586E-02	3.10E+00	6.11E-02	1.31E+02	0.00E+00	0.00E+00	1.34E+02	1.31E+02
82 L1	1.586E-02	3.10E+00	6.11E-02	1.52E+02	0.00E+00	0.00E+00	1.55E+02	1.52E+02
	2.000E-02	2.34E+00	6.90E-02	8.40E+01	0.00E+00	0.00E+00	8.64E+01	8.40E+01
	3.000E-02	1.38E+00	8.23E-02	2.89E+01	0.00E+00	0.00E+00	3.03E+01	2.89E+01
	4.000E-02	9.20E-01	9.02E-02	1.33E+01	0.00E+00	0.00E+00	1.44E+01	1.34E+01
	5.000E-02	6.55E-01	9.48E-02	7.29E+00	0.00E+00	0.00E+00	8.04E+00	7.39E+00
	6.000E-02	4.90E-01	9.73E-02	4.43E+00	0.00E+00	0.00E+00	5.02E+00	4.53E+00
	8.000E-02	3.08E-01	9.92E-02	2.01E+00	0.00E+00	0.00E+00	2.42E+00	2.11E+00
	8.800E-02	2.63E-01	9.93E-02	1.55E+00	0.00E+00	0.00E+00	1.91E+00	1.65E+00

Figure A.1: Mass attenuation coefficients for lead - 1.

82 K	8.800E-02	2.63E-01	9.93E-02	7.32E+00	0.00E+00	0.00E+00	7.68E+00	7.42E+00
	1.000E-01	2.13E-01	9.89E-02	5.24E+00	0.00E+00	0.00E+00	5.55E+00	5.34E+00
	1.500E-01	1.05E-01	9.48E-02	1.81E+00	0.00E+00	0.00E+00	2.01E+00	1.91E+00
	2.000E-01	6.26E-02	8.97E-02	8.46E-01	0.00E+00	0.00E+00	9.99E-01	9.36E-01
	3.000E-01	2.99E-02	8.04E-02	2.93E-01	0.00E+00	0.00E+00	4.03E-01	3.73E-01
	4.000E-01	1.75E-02	7.31E-02	1.42E-01	0.00E+00	0.00E+00	2.32E-01	2.15E-01
	5.000E-01	1.14E-02	6.73E-02	8.26E-02	0.00E+00	0.00E+00	1.61E-01	1.50E-01
	6.000E-01	8.06E-03	6.26E-02	5.41E-02	0.00E+00	0.00E+00	1.25E-01	1.17E-01
	8.000E-01	4.62E-03	5.54E-02	2.87E-02	0.00E+00	0.00E+00	8.87E-02	8.41E-02
	1.000E+00	2.99E-03	4.99E-02	1.81E-02	0.00E+00	0.00E+00	7.10E-02	6.80E-02
	1.022E+00	2.87E-03	4.94E-02	1.73E-02	0.00E+00	0.00E+00	6.96E-02	6.68E-02
	1.250E+00	1.93E-03	4.48E-02	1.17E-02	3.78E-04	0.00E+00	5.88E-02	5.68E-02
	1.500E+00	1.35E-03	4.07E-02	8.32E-03	1.81E-03	0.00E+00	5.22E-02	5.09E-02
	2.000E+00	7.63E-04	3.48E-02	5.03E-03	5.45E-03	0.00E+00	4.61E-02	4.53E-02
	2.044E+00	7.30E-04	3.44E-02	4.85E-03	5.77E-03	0.00E+00	4.58E-02	4.50E-02
	3.000E+00	3.41E-04	2.74E-02	2.63E-03	1.19E-02	9.59E-06	4.23E-02	4.20E-02
	4.000E+00	1.92E-04	2.29E-02	1.72E-03	1.71E-02	3.91E-05	4.20E-02	4.18E-02
	5.000E+00	1.23E-04	1.98E-02	1.26E-03	2.15E-02	7.77E-05	4.27E-02	4.26E-02
	6.000E+00	8.54E-05	1.75E-02	9.89E-04	2.52E-02	1.19E-04	4.39E-02	4.38E-02
	7.000E+00	6.28E-05	1.57E-02	8.10E-04	2.85E-02	1.60E-04	4.53E-02	4.52E-02
	8.000E+00	4.81E-05	1.43E-02	6.84E-04	3.15E-02	2.00E-04	4.67E-02	4.67E-02
	9.000E+00	3.80E-05	1.32E-02	5.91E-04	3.42E-02	2.38E-04	4.82E-02	4.82E-02
	1.000E+01	3.08E-05	1.22E-02	5.20E-04	3.67E-02	2.74E-04	4.97E-02	4.97E-02
	1.100E+01	2.54E-05	1.14E-02	4.64E-04	3.90E-02	3.08E-04	5.12E-02	5.11E-02
	1.200E+01	2.14E-05	1.07E-02	4.19E-04	4.12E-02	3.40E-04	5.26E-02	5.26E-02
	1.300E+01	1.82E-05	1.00E-02	3.81E-04	4.32E-02	3.70E-04	5.40E-02	5.40E-02
	1.400E+01	1.57E-05	9.50E-03	3.50E-04	4.50E-02	3.99E-04	5.53E-02	5.53E-02
	1.500E+01	1.37E-05	9.02E-03	3.23E-04	4.68E-02	4.26E-04	5.66E-02	5.66E-02
	1.600E+01	1.20E-05	8.59E-03	3.00E-04	4.84E-02	4.51E-04	5.78E-02	5.78E-02
	1.800E+01	9.50E-06	7.85E-03	2.63E-04	5.14E-02	4.98E-04	6.00E-02	6.00E-02
	2.000E+01	7.70E-06	7.24E-03	2.33E-04	5.40E-02	5.41E-04	6.21E-02	6.20E-02
	2.200E+01	6.36E-06	6.73E-03	2.10E-04	5.64E-02	5.80E-04	6.39E-02	6.39E-02
	2.400E+01	5.34E-06	6.29E-03	1.91E-04	5.86E-02	6.16E-04	6.57E-02	6.57E-02
	2.600E+01	4.55E-06	5.90E-03	1.75E-04	6.06E-02	6.49E-04	6.73E-02	6.73E-02
	2.800E+01	3.93E-06	5.57E-03	1.61E-04	6.24E-02	6.80E-04	6.88E-02	6.88E-02
	3.000E+01	3.42E-06	5.27E-03	1.50E-04	6.41E-02	7.08E-04	7.02E-02	7.02E-02
	4.000E+01	1.92E-06	4.19E-03	1.10E-04	7.10E-02	8.25E-04	7.61E-02	7.61E-02
	5.000E+01	1.23E-06	3.50E-03	8.70E-05	7.61E-02	9.12E-04	8.06E-02	8.06E-02
	6.000E+01	8.55E-07	3.01E-03	7.19E-05	8.00E-02	9.81E-04	8.41E-02	8.41E-02
	8.000E+01	4.81E-07	2.38E-03	5.34E-05	8.58E-02	1.08E-03	8.93E-02	8.93E-02
	1.000E+02	3.08E-07	1.97E-03	4.24E-05	8.99E-02	1.16E-03	9.31E-02	9.31E-02
	1.500E+02	1.37E-07	1.40E-03	2.81E-05	9.64E-02	1.28E-03	9.91E-02	9.91E-02
	2.000E+02	7.70E-08	1.10E-03	2.10E-05	1.00E-01	1.35E-03	1.03E-01	1.03E-01
	3.000E+02	3.42E-08	7.81E-04	1.39E-05	1.05E-01	1.44E-03	1.07E-01	1.07E-01
	4.000E+02	1.92E-08	6.11E-04	1.04E-05	1.07E-01	1.50E-03	1.09E-01	1.09E-01
	5.000E+02	1.23E-08	5.06E-04	8.32E-06	1.09E-01	1.53E-03	1.11E-01	1.11E-01
	6.000E+02	8.55E-09	4.33E-04	6.93E-06	1.10E-01	1.56E-03	1.12E-01	1.12E-01
	8.000E+02	4.81E-09	3.38E-04	5.19E-06	1.12E-01	1.60E-03	1.14E-01	1.14E-01
	1.000E+03	3.08E-09	2.78E-04	4.15E-06	1.13E-01	1.62E-03	1.15E-01	1.15E-01
	1.500E+03	1.37E-09	1.94E-04	2.76E-06	1.14E-01	1.65E-03	1.16E-01	1.16E-01
	2.000E+03	7.70E-10	1.50E-04	2.07E-06	1.15E-01	1.67E-03	1.17E-01	1.17E-01
	3.000E+03	3.42E-10	1.05E-04	1.38E-06	1.16E-01	1.70E-03	1.18E-01	1.18E-01
	4.000E+03	1.92E-10	8.08E-05	1.04E-06	1.16E-01	1.71E-03	1.18E-01	1.18E-01
	5.000E+03	1.23E-10	6.60E-05	8.28E-07	1.17E-01	1.72E-03	1.18E-01	1.18E-01
	6.000E+03	8.55E-11	5.60E-05	6.90E-07	1.17E-01	1.72E-03	1.19E-01	1.19E-01
	8.000E+03	4.81E-11	4.31E-05	5.18E-07	1.17E-01	1.73E-03	1.19E-01	1.19E-01
	1.000E+04	3.08E-11	3.52E-05	4.14E-07	1.17E-01	1.73E-03	1.19E-01	1.19E-01
	1.500E+04	1.37E-11	2.43E-05	2.76E-07	1.17E-01	1.74E-03	1.19E-01	1.19E-01
	2.000E+04	7.70E-12	1.87E-05	2.07E-07	1.18E-01	1.74E-03	1.19E-01	1.19E-01
	3.000E+04	3.42E-12	1.29E-05	1.38E-07	1.18E-01	1.75E-03	1.20E-01	1.20E-01
	4.000E+04	1.92E-12	9.91E-06	1.03E-07	1.18E-01	1.75E-03	1.20E-01	1.20E-01

Figure A.2: Mass attenuation coefficients for lead - 2.

XCOM:

Constituents (Atomic Number : Fraction by Weight)

Z=6 : 1.000000

PHOTON ENERGY (MeV)	SCATTERING COHERENT (cm2/g)	SCATTERING INCOHER. (cm2/g)	PHOTO-ELECTRIC ABSORPTION (cm2/g)	PAIR PRODUCTION IN NUCLEAR FIELD (cm2/g)	PAIR PRODUCTION IN ELECTRON FIELD (cm2/g)	TOTAL ATTENUATION WITH COHERENT SCATT. (cm2/g)	TOTAL ATTENUATION WITHOUT COHERENT SCATT. (cm2/g)
1.000E-03	1.08E+00	1.26E-02	2.21E+03	0.00E+00	0.00E+00	2.21E+03	2.21E+03
1.500E-03	9.59E-01	2.51E-02	6.99E+02	0.00E+00	0.00E+00	7.00E+02	6.99E+02
2.000E-03	8.32E-01	3.86E-02	3.02E+02	0.00E+00	0.00E+00	3.03E+02	3.02E+02
3.000E-03	6.13E-01	6.41E-02	8.96E+01	0.00E+00	0.00E+00	9.03E+01	8.97E+01
4.000E-03	4.60E-01	8.45E-02	3.72E+01	0.00E+00	0.00E+00	3.78E+01	3.73E+01
5.000E-03	3.59E-01	9.95E-02	1.87E+01	0.00E+00	0.00E+00	1.91E+01	1.88E+01
6.000E-03	2.92E-01	1.10E-01	1.05E+01	0.00E+00	0.00E+00	1.09E+01	1.07E+01
8.000E-03	2.10E-01	1.25E-01	4.24E+00	0.00E+00	0.00E+00	4.58E+00	4.37E+00
1.000E-02	1.62E-01	1.35E-01	2.08E+00	0.00E+00	0.00E+00	2.37E+00	2.21E+00
1.500E-02	9.79E-02	1.51E-01	5.59E-01	0.00E+00	0.00E+00	8.07E-01	7.10E-01
2.000E-02	6.48E-02	1.60E-01	2.18E-01	0.00E+00	0.00E+00	4.42E-01	3.77E-01
3.000E-02	3.36E-02	1.65E-01	5.71E-02	0.00E+00	0.00E+00	2.56E-01	2.23E-01
4.000E-02	2.05E-02	1.65E-01	2.19E-02	0.00E+00	0.00E+00	2.08E-01	1.87E-01
5.000E-02	1.37E-02	1.63E-01	1.04E-02	0.00E+00	0.00E+00	1.87E-01	1.73E-01
6.000E-02	9.81E-03	1.60E-01	5.67E-03	0.00E+00	0.00E+00	1.75E-01	1.66E-01
8.000E-02	5.71E-03	1.53E-01	2.17E-03	0.00E+00	0.00E+00	1.61E-01	1.55E-01
1.000E-01	3.72E-03	1.47E-01	1.03E-03	0.00E+00	0.00E+00	1.51E-01	1.48E-01
1.500E-01	1.68E-03	1.33E-01	2.71E-04	0.00E+00	0.00E+00	1.35E-01	1.33E-01
2.000E-01	9.54E-04	1.22E-01	1.06E-04	0.00E+00	0.00E+00	1.23E-01	1.22E-01
3.000E-01	4.26E-04	1.06E-01	2.98E-05	0.00E+00	0.00E+00	1.07E-01	1.06E-01
4.000E-01	2.40E-04	9.52E-02	1.27E-05	0.00E+00	0.00E+00	9.55E-02	9.52E-02
5.000E-01	1.54E-04	8.70E-02	6.84E-06	0.00E+00	0.00E+00	8.72E-02	8.70E-02
6.000E-01	1.07E-04	8.05E-02	4.25E-06	0.00E+00	0.00E+00	8.06E-02	8.05E-02
8.000E-01	6.02E-05	7.07E-02	2.14E-06	0.00E+00	0.00E+00	7.08E-02	7.07E-02
1.000E+00	3.85E-05	6.36E-02	1.33E-06	0.00E+00	0.00E+00	6.36E-02	6.36E-02
1.022E+00	3.69E-05	6.29E-02	1.23E-06	0.00E+00	0.00E+00	6.30E-02	6.29E-02
1.250E+00	2.47E-05	5.69E-02	8.35E-07	1.44E-05	0.00E+00	5.69E-02	5.69E-02
1.500E+00	1.71E-05	5.17E-02	6.06E-07	7.99E-05	0.00E+00	5.18E-02	5.18E-02
2.000E+00	9.63E-06	4.41E-02	3.83E-07	3.19E-04	0.00E+00	4.44E-02	4.44E-02
2.044E+00	9.22E-06	4.36E-02	3.70E-07	3.44E-04	0.00E+00	4.39E-02	4.39E-02
3.000E+00	4.28E-06	3.47E-02	2.15E-07	9.13E-04	1.21E-05	3.56E-02	3.56E-02
4.000E+00	2.41E-06	2.89E-02	1.48E-07	1.48E-03	4.96E-05	3.05E-02	3.05E-02
5.000E+00	1.54E-06	2.50E-02	1.12E-07	1.99E-03	9.88E-05	2.71E-02	2.71E-02
6.000E+00	1.07E-06	2.21E-02	9.03E-08	2.44E-03	1.52E-04	2.47E-02	2.47E-02
7.000E+00	7.86E-07	1.99E-02	7.56E-08	2.85E-03	2.05E-04	2.29E-02	2.29E-02
8.000E+00	6.02E-07	1.81E-02	6.49E-08	3.22E-03	2.56E-04	2.15E-02	2.15E-02
9.000E+00	4.76E-07	1.66E-02	5.69E-08	3.55E-03	3.05E-04	2.05E-02	2.05E-02
1.000E+01	3.85E-07	1.54E-02	5.06E-08	3.85E-03	3.52E-04	1.96E-02	1.96E-02
1.100E+01	3.18E-07	1.44E-02	4.55E-08	4.13E-03	3.96E-04	1.89E-02	1.89E-02
1.200E+01	2.68E-07	1.35E-02	4.14E-08	4.38E-03	4.38E-04	1.83E-02	1.83E-02
1.300E+01	2.28E-07	1.27E-02	3.80E-08	4.62E-03	4.78E-04	1.78E-02	1.78E-02
1.400E+01	1.97E-07	1.20E-02	3.50E-08	4.84E-03	5.16E-04	1.74E-02	1.74E-02
1.500E+01	1.71E-07	1.14E-02	3.25E-08	5.04E-03	5.53E-04	1.70E-02	1.70E-02
1.600E+01	1.51E-07	1.08E-02	3.04E-08	5.23E-03	5.87E-04	1.67E-02	1.67E-02
1.800E+01	1.19E-07	9.91E-03	2.68E-08	5.59E-03	6.51E-04	1.61E-02	1.61E-02
2.000E+01	9.63E-08	9.14E-03	2.40E-08	5.90E-03	7.09E-04	1.58E-02	1.58E-02

Figure A.3: Mass attenuation coefficients for Carbon - 1.

2.200E+01	7.96E-08	8.49E-03	2.17E-08	6.19E-03	7.64E-04	1.54E-02	1.54E-02
2.400E+01	6.69E-08	7.94E-03	1.98E-08	6.45E-03	8.14E-04	1.52E-02	1.52E-02
2.600E+01	5.70E-08	7.45E-03	1.82E-08	6.69E-03	8.60E-04	1.50E-02	1.50E-02
2.800E+01	4.92E-08	7.03E-03	1.69E-08	6.91E-03	9.03E-04	1.48E-02	1.48E-02
3.000E+01	4.28E-08	6.65E-03	1.57E-08	7.12E-03	9.44E-04	1.47E-02	1.47E-02
4.000E+01	2.41E-08	5.29E-03	1.17E-08	7.96E-03	1.12E-03	1.44E-02	1.44E-02
5.000E+01	1.54E-08	4.41E-03	9.28E-09	8.59E-03	1.25E-03	1.43E-02	1.43E-02
6.000E+01	1.07E-08	3.80E-03	7.71E-09	9.10E-03	1.36E-03	1.43E-02	1.43E-02
8.000E+01	6.02E-09	3.00E-03	5.76E-09	9.86E-03	1.52E-03	1.44E-02	1.44E-02
1.000E+02	3.85E-09	2.49E-03	4.59E-09	1.04E-02	1.65E-03	1.46E-02	1.46E-02
1.500E+02	1.71E-09	1.77E-03	3.05E-09	1.14E-02	1.87E-03	1.50E-02	1.50E-02
2.000E+02	9.63E-10	1.39E-03	2.28E-09	1.20E-02	2.02E-03	1.54E-02	1.54E-02
3.000E+02	4.28E-10	9.85E-04	1.52E-09	1.27E-02	2.20E-03	1.59E-02	1.59E-02
4.000E+02	2.41E-10	7.72E-04	1.14E-09	1.31E-02	2.32E-03	1.62E-02	1.62E-02
5.000E+02	1.54E-10	6.39E-04	9.10E-10	1.34E-02	2.40E-03	1.64E-02	1.64E-02
6.000E+02	1.07E-10	5.47E-04	7.58E-10	1.36E-02	2.46E-03	1.66E-02	1.66E-02
8.000E+02	6.02E-11	4.27E-04	5.68E-10	1.39E-02	2.55E-03	1.69E-02	1.69E-02
1.000E+03	3.85E-11	3.51E-04	4.55E-10	1.41E-02	2.61E-03	1.70E-02	1.70E-02
1.500E+03	1.71E-11	2.45E-04	3.03E-10	1.43E-02	2.69E-03	1.73E-02	1.73E-02
2.000E+03	9.63E-12	1.90E-04	2.27E-10	1.45E-02	2.74E-03	1.74E-02	1.74E-02
3.000E+03	4.28E-12	1.32E-04	1.51E-10	1.47E-02	2.80E-03	1.76E-02	1.76E-02
4.000E+03	2.41E-12	1.02E-04	1.14E-10	1.47E-02	2.83E-03	1.77E-02	1.77E-02
5.000E+03	1.54E-12	8.34E-05	9.08E-11	1.48E-02	2.85E-03	1.77E-02	1.77E-02
6.000E+03	1.07E-12	7.07E-05	7.57E-11	1.48E-02	2.86E-03	1.78E-02	1.78E-02
8.000E+03	6.02E-13	5.45E-05	5.68E-11	1.49E-02	2.88E-03	1.78E-02	1.78E-02
1.000E+04	3.85E-13	4.45E-05	4.54E-11	1.49E-02	2.89E-03	1.79E-02	1.79E-02
1.500E+04	1.71E-13	3.07E-05	3.03E-11	1.50E-02	2.91E-03	1.79E-02	1.79E-02
2.000E+04	9.63E-14	2.36E-05	2.27E-11	1.50E-02	2.92E-03	1.79E-02	1.79E-02
3.000E+04	4.28E-14	1.63E-05	1.51E-11	1.50E-02	2.93E-03	1.80E-02	1.80E-02
4.000E+04	2.41E-14	1.25E-05	1.14E-11	1.50E-02	2.94E-03	1.80E-02	1.80E-02
5.000E+04	1.54E-14	1.02E-05	9.08E-12	1.50E-02	2.94E-03	1.80E-02	1.80E-02
6.000E+04	1.07E-14	8.61E-06	7.57E-12	1.50E-02	2.94E-03	1.80E-02	1.80E-02
8.000E+04	6.02E-15	6.60E-06	5.68E-12	1.50E-02	2.94E-03	1.80E-02	1.80E-02
1.000E+05	3.85E-15	5.37E-06	4.54E-12	1.51E-02	2.94E-03	1.80E-02	1.80E-02

Return to selection page.

Figure A.4: Mass attenuation coefficients for Carbon - 2.

XCOM:

Constituents (Atomic Number : Fraction by Weight)

Z=1 : 1.000000

PHOTON ENERGY (MeV)	SCATTERING COHERENT (cm2/g)	SCATTERING INCOHER. (cm2/g)	PHOTO- ELECTRIC ABSORPTION (cm2/g)	PAIR PRODUCTION IN NUCLEAR FIELD (cm2/g)	PAIR PRODUCTION IN ELECTRON FIELD (cm2/g)	TOTAL ATTENUATION WITH COHERENT SCATT. (cm2/g)	TOTAL ATTENUATION WITHOUT COHERENT SCATT. (cm2/g)
1.000E-03	3.47E-01	5.03E-02	6.82E+00	0.00E+00	0.00E+00	7.21E+00	6.87E+00
1.500E-03	2.98E-01	9.86E-02	1.75E+00	0.00E+00	0.00E+00	2.15E+00	1.85E+00
2.000E-03	2.47E-01	1.48E-01	6.64E-01	0.00E+00	0.00E+00	1.06E+00	8.12E-01
3.000E-03	1.65E-01	2.28E-01	1.68E-01	0.00E+00	0.00E+00	5.61E-01	3.96E-01
4.000E-03	1.12E-01	2.79E-01	6.29E-02	0.00E+00	0.00E+00	4.55E-01	3.42E-01
5.000E-03	8.01E-02	3.10E-01	2.93E-02	0.00E+00	0.00E+00	4.19E-01	3.39E-01
6.000E-03	5.97E-02	3.29E-01	1.57E-02	0.00E+00	0.00E+00	4.04E-01	3.44E-01
8.000E-03	3.66E-02	3.49E-01	5.86E-03	0.00E+00	0.00E+00	3.91E-01	3.55E-01
1.000E-02	2.46E-02	3.58E-01	2.72E-03	0.00E+00	0.00E+00	3.85E-01	3.61E-01
1.500E-02	1.16E-02	3.64E-01	6.74E-04	0.00E+00	0.00E+00	3.76E-01	3.65E-01
2.000E-02	6.69E-03	3.63E-01	2.50E-04	0.00E+00	0.00E+00	3.69E-01	3.63E-01
3.000E-02	3.02E-03	3.54E-01	6.17E-05	0.00E+00	0.00E+00	3.57E-01	3.54E-01
4.000E-02	1.71E-03	3.44E-01	2.28E-05	0.00E+00	0.00E+00	3.46E-01	3.44E-01
5.000E-02	1.10E-03	3.34E-01	1.06E-05	0.00E+00	0.00E+00	3.36E-01	3.34E-01
6.000E-02	7.65E-04	3.25E-01	5.65E-06	0.00E+00	0.00E+00	3.26E-01	3.25E-01
8.000E-02	4.31E-04	3.09E-01	2.10E-06	0.00E+00	0.00E+00	3.09E-01	3.09E-01
1.000E-01	2.76E-04	2.94E-01	9.82E-07	0.00E+00	0.00E+00	2.94E-01	2.94E-01
1.500E-01	1.23E-04	2.65E-01	2.50E-07	0.00E+00	0.00E+00	2.65E-01	2.65E-01
2.000E-01	6.91E-05	2.43E-01	9.63E-08	0.00E+00	0.00E+00	2.43E-01	2.43E-01
3.000E-01	3.07E-05	2.11E-01	2.64E-08	0.00E+00	0.00E+00	2.11E-01	2.11E-01
4.000E-01	1.73E-05	1.89E-01	1.11E-08	0.00E+00	0.00E+00	1.89E-01	1.89E-01
5.000E-01	1.11E-05	1.73E-01	5.93E-09	0.00E+00	0.00E+00	1.73E-01	1.73E-01
6.000E-01	7.68E-06	1.60E-01	3.68E-09	0.00E+00	0.00E+00	1.60E-01	1.60E-01
8.000E-01	4.32E-06	1.40E-01	1.86E-09	0.00E+00	0.00E+00	1.40E-01	1.40E-01
1.000E+00	2.76E-06	1.26E-01	1.17E-09	0.00E+00	0.00E+00	1.26E-01	1.26E-01
1.022E+00	2.65E-06	1.25E-01	1.12E-09	0.00E+00	0.00E+00	1.25E-01	1.25E-01
1.250E+00	1.77E-06	1.13E-01	7.79E-10	4.66E-06	0.00E+00	1.13E-01	1.13E-01
1.500E+00	1.23E-06	1.03E-01	5.81E-10	2.62E-05	0.00E+00	1.03E-01	1.03E-01
2.000E+00	6.91E-07	8.76E-02	3.70E-10	1.05E-04	0.00E+00	8.77E-02	8.77E-02
2.044E+00	6.61E-07	8.65E-02	3.59E-10	1.13E-04	0.00E+00	8.66E-02	8.66E-02
3.000E+00	3.07E-07	6.89E-02	2.11E-10	3.02E-04	2.41E-05	6.92E-02	6.92E-02
4.000E+00	1.73E-07	5.75E-02	1.46E-10	4.90E-04	9.84E-05	5.81E-02	5.81E-02
5.000E+00	1.11E-07	4.96E-02	1.11E-10	6.58E-04	1.96E-04	5.05E-02	5.05E-02
6.000E+00	7.68E-08	4.39E-02	9.01E-11	8.10E-04	3.01E-04	4.50E-02	4.50E-02
7.000E+00	5.64E-08	3.94E-02	7.55E-11	9.44E-04	4.06E-04	4.08E-02	4.08E-02
8.000E+00	4.32E-08	3.59E-02	6.50E-11	1.07E-03	5.08E-04	3.75E-02	3.75E-02
9.000E+00	3.41E-08	3.30E-02	5.70E-11	1.18E-03	6.06E-04	3.48E-02	3.48E-02
1.000E+01	2.76E-08	3.06E-02	5.08E-11	1.28E-03	6.99E-04	3.25E-02	3.25E-02
1.100E+01	2.28E-08	2.85E-02	4.58E-11	1.37E-03	7.87E-04	3.07E-02	3.07E-02
1.200E+01	1.92E-08	2.67E-02	4.17E-11	1.45E-03	8.71E-04	2.91E-02	2.91E-02
1.300E+01	1.64E-08	2.52E-02	3.82E-11	1.53E-03	9.50E-04	2.77E-02	2.77E-02
1.400E+01	1.41E-08	2.38E-02	3.53E-11	1.61E-03	1.03E-03	2.65E-02	2.65E-02
1.500E+01	1.23E-08	2.26E-02	3.28E-11	1.67E-03	1.10E-03	2.54E-02	2.54E-02
1.600E+01	1.08E-08	2.15E-02	3.07E-11	1.74E-03	1.17E-03	2.45E-02	2.45E-02
1.800E+01	8.53E-09	1.97E-02	2.71E-11	1.86E-03	1.29E-03	2.28E-02	2.28E-02
2.000E+01	6.91E-09	1.82E-02	2.42E-11	1.97E-03	1.41E-03	2.15E-02	2.15E-02

Figure A.5: Mass attenuation coefficients for Hydrogen - 1.

2.200E+01	5.71E-09	1.69E-02	2.19E-11	2.07E-03	1.52E-03	2.04E-02	2.04E-02
2.400E+01	4.80E-09	1.58E-02	2.00E-11	2.16E-03	1.62E-03	1.95E-02	1.95E-02
2.600E+01	4.09E-09	1.48E-02	1.84E-11	2.24E-03	1.71E-03	1.87E-02	1.87E-02
2.800E+01	3.52E-09	1.40E-02	1.71E-11	2.32E-03	1.80E-03	1.81E-02	1.81E-02
3.000E+01	3.07E-09	1.32E-02	1.59E-11	2.39E-03	1.88E-03	1.75E-02	1.75E-02
4.000E+01	1.73E-09	1.05E-02	1.18E-11	2.69E-03	2.22E-03	1.54E-02	1.54E-02
5.000E+01	1.11E-09	8.77E-03	9.42E-12	2.93E-03	2.49E-03	1.42E-02	1.42E-02
6.000E+01	7.67E-10	7.55E-03	7.83E-12	3.12E-03	2.72E-03	1.34E-02	1.34E-02
8.000E+01	4.31E-10	5.96E-03	5.85E-12	3.42E-03	3.07E-03	1.25E-02	1.25E-02
1.000E+02	2.76E-10	4.94E-03	4.67E-12	3.65E-03	3.34E-03	1.19E-02	1.19E-02
1.500E+02	1.23E-10	3.52E-03	3.10E-12	4.05E-03	3.83E-03	1.14E-02	1.14E-02
2.000E+02	6.90E-11	2.76E-03	2.32E-12	4.31E-03	4.17E-03	1.12E-02	1.12E-02
3.000E+02	3.07E-11	1.96E-03	1.55E-12	4.63E-03	4.62E-03	1.12E-02	1.12E-02
4.000E+02	1.73E-11	1.53E-03	1.16E-12	4.83E-03	4.91E-03	1.13E-02	1.13E-02
5.000E+02	1.10E-11	1.27E-03	9.26E-13	4.96E-03	5.12E-03	1.14E-02	1.14E-02
6.000E+02	7.67E-12	1.09E-03	7.71E-13	5.06E-03	5.28E-03	1.14E-02	1.14E-02
8.000E+02	4.31E-12	8.48E-04	5.78E-13	5.19E-03	5.51E-03	1.15E-02	1.15E-02
1.000E+03	2.76E-12	6.98E-04	4.63E-13	5.27E-03	5.67E-03	1.16E-02	1.16E-02
1.500E+03	1.23E-12	4.87E-04	3.08E-13	5.40E-03	5.91E-03	1.18E-02	1.18E-02
2.000E+03	6.90E-13	3.77E-04	2.31E-13	5.47E-03	6.05E-03	1.19E-02	1.19E-02
3.000E+03	3.07E-13	2.62E-04	1.54E-13	5.54E-03	6.20E-03	1.20E-02	1.20E-02
4.000E+03	1.73E-13	2.02E-04	1.16E-13	5.59E-03	6.29E-03	1.21E-02	1.21E-02
5.000E+03	1.10E-13	1.66E-04	9.25E-14	5.61E-03	6.35E-03	1.21E-02	1.21E-02
6.000E+03	7.67E-14	1.40E-04	7.71E-14	5.63E-03	6.39E-03	1.22E-02	1.22E-02
8.000E+03	4.31E-14	1.08E-04	5.78E-14	5.66E-03	6.45E-03	1.22E-02	1.22E-02
1.000E+04	2.76E-14	8.83E-05	4.62E-14	5.67E-03	6.48E-03	1.22E-02	1.22E-02
1.500E+04	1.23E-14	6.10E-05	3.08E-14	5.69E-03	6.53E-03	1.23E-02	1.23E-02
2.000E+04	6.90E-15	4.69E-05	2.31E-14	5.71E-03	6.55E-03	1.23E-02	1.23E-02
3.000E+04	3.07E-15	3.24E-05	1.54E-14	5.72E-03	6.58E-03	1.23E-02	1.23E-02
4.000E+04	1.73E-15	2.48E-05	1.16E-14	5.72E-03	6.60E-03	1.24E-02	1.24E-02
5.000E+04	1.10E-15	2.02E-05	9.24E-15	5.73E-03	6.61E-03	1.24E-02	1.24E-02
6.000E+04	7.67E-16	1.71E-05	7.70E-15	5.73E-03	6.62E-03	1.24E-02	1.24E-02
8.000E+04	4.31E-16	1.31E-05	5.78E-15	5.73E-03	6.63E-03	1.24E-02	1.24E-02
1.000E+05	2.76E-16	1.07E-05	4.62E-15	5.74E-03	6.63E-03	1.24E-02	1.24E-02

Return to selection page.

Figure A.6: Mass attenuation coefficients for Hydrogen - 2.

Appendix B.
Manabe results for other configurations

Table B.1 and Table B.2 show the sampling fluctuation contributions to the photon inefficiency for the 0.5mm Pb/5mm scintillator and 0.1mm Pb/5mm scintillator counters according to Manabe[19].

Table B.1: Photon inefficiency in a 0.5mm Pb/5mm scintillator sandwich counter due to sampling fluctuations calculated by Manabe[19]. The thresholds are in terms of visible energy.

photon energy (MeV)	Inefficiency th 0.4 MeV ($\times 10^{-4}$)	Inefficiency th 1.0 MeV ($\times 10^{-4}$)	Inefficiency th 3.0 MeV ($\times 10^{-4}$)	Inefficiency th 5.0 MeV ($\times 10^{-4}$)
20	0.062	0.29	2.58	30.9
30	0.030	0.099	0.44	1.26
40	0.011	0.052	0.19	0.42
50	0.020	0.036	0.07	0.17
70	0.0024	0.0073	0.032	0.046
100	0.0025	0.0025	0.0074	0.015

Table B.2: Photon inefficiency in a 0.1mm Pb/5mm scintillator sandwich counter due to sampling fluctuations calculated by Manabe[19]. The thresholds are in terms of visible energy.

photon energy (MeV)	Inefficiency th 0.4 MeV ($\times 10^{-4}$)	Inefficiency th 1.0 MeV ($\times 10^{-4}$)	Inefficiency th 3.0 MeV ($\times 10^{-4}$)	Inefficiency th 5.0 MeV ($\times 10^{-4}$)
20	0.050	0.11	0.29	0.49
30	0.020	0.043	0.12	0.17
40	0.010	0.013	0.070	0.13
50	0.005	0.007	0.039	0.062
70	0.0025	0.0057	0.022	0.030
100	0	0	0	0.025

Appendix C.
Additional Kurebayashi results for photonuclear inefficiency

Table C.1 contains photonuclear inefficiency data from the Kurebayashi[7] thesis.

Table C.1: Photon inefficiency due to photonuclear interactions from the Kurebayashi thesis. Threshold was 1 MeV in total deposited energy.

photon energy (MeV)	Inefficiency 1/5mm Pb/scint ($\times 10^{-5}$)	Inefficiency 0.5/5mm Pb/scint ($\times 10^{-5}$)
54-91	$20.0^{+24.1}_{-20.0}$	$6.89^{+7.69}_{-6.89}$
91-129	$2.58^{+1.32}_{-1.33}$	$1.68^{+1.59}_{-1.47}$
129-167	$4.99^{+3.02}_{-3.40}$	$1.71^{+2.57}_{-1.71}$
167-204	$1.78^{+1.00}_{-1.10}$	$0.77^{+0.56}_{-0.55}$

Fig. C.1 shows the photonuclear component of the inefficiency of 1mm/5mm Pb/scint and 0.5mm/5mm Pb/scint sandwich counters as a function of threshold for various incident photon energy ranges. Note that the thresholds are on total energy deposited. To transform to visible energy multiply the 1mm/5mm values by ~ 0.3 and the 0.5mm/5mm values by ~ 0.5.

Fig. C.2 shows the ratio of the 0.5mm Pb/ 5mm scintillator photonuclear inefficiency to that of the 1mm Pb/ 5mm scintillator structure as a function of incident photon energy and threshold. It's not completely simple to conclude that the 0.5mm/5mm structure has a lower photonuclear inefficiency than the 1mm/5mm structure. However one should keep in mind that thresholds are actually set in terms of visible energy, not the total deposited energy used in these results. Therefore, for example, a 5 MeV deposited energy threshold for the 1mm/5mm case corresponds to the same visible energy as for a 3 MeV deposited energy threshold for the 0.5/5mm case.

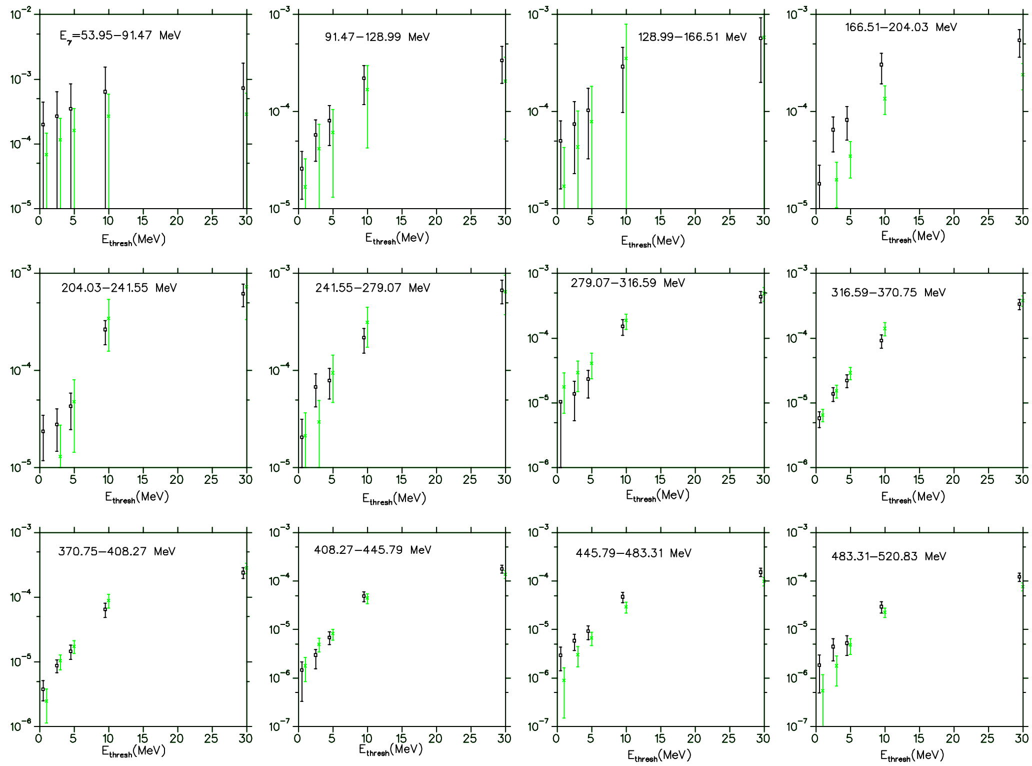

Figure C.1: Photonuclear inefficiency of Pb/scintillator sandwich counters as a function of threshold energy for bins of incident photon energy. Black squares are for an 18.4 X_0 1mm/5mm structure, green X's for 6.8 X_0 of 0.5mm/5mm structure followed by 18.4 X_0 of 1mm/5mm. **Note that the thresholds are on total energy deposited, not visible energy.**

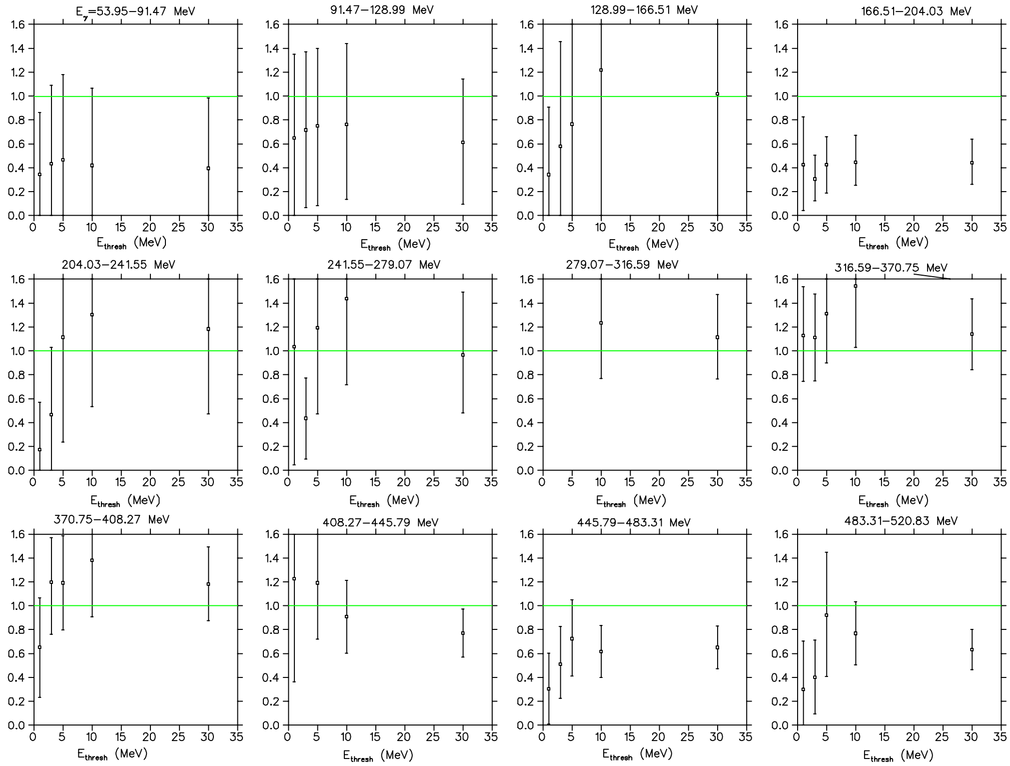

Figure C.2: Ratio of photonuclear inefficiency of 0.5mm Pb/ 5mm scintillator sandwich counters to that of a 1mm Pb/ 5mm scintillator counter as a function of threshold energy for bins of incident photon energy. **Note that the thresholds are on total energy deposited, not visible energy.**

Appendix D.
A note of caution about the INS results

This is really a note of caution about my extraction of these results, given my inability to read Japanese. However, I should also mention that the evolution of analysis mentioned above seem to result in quite different values for the measured photon nuclear inefficiencies. Table D.1 gives a couple of examples.

Table D.1: Photon inefficiency in CsI from various sources Threshold was 10 MeV in total deposited energy.

Source	E_γ (MeV)	Inefficiency ($\times 10^{-5}$)
Watanabe Thesis	134.2	$1.64^{+0.29}_{-0.04}$
Watanabe Thesis	175.4	$1.00^{+0.18}_{-0.03}$
Mori Thesis	90-170	11.0 ± 2.0
Watanabe Reanalysis	120-180	12.3 ± 1.5
Watanabe Reanalysis	182-240	10.2 ± 1.2

References

1. T. Nakano and Y. Kuno, "A Study on Photon Detection Efficiency Using Real $K_{\pi 2}$ Data", E787 TN 256, 24 July 1993.
2. T. Sasaki, "Photon detection inefficiency measurements using tagged photons from the decay $K^+ \to \pi^+\pi^0$", Osaka University Masters Thesis, 6 Feb 1997.
3. S. Ajimura, et al., "Measurements of the photon detection inefficiency of calorimeters between 185 and 505 MeV", NIM **A 435** (1999) 408.
4. http://physics.nist/gov/PhysRefData/Xcom/Text/XCOM.html.
5. "Bicron Premium Plastic and Liquid Scintillators", 1974.
6. K. Mori, "Measurement of Inefficiency of photo-nuclear interaction with CsI photon counter", Osaka Masters Thesis, Feb 1999.
7. K. Kurebayashi, "Measurement of Inefficiency of photo-nuclear interaction with lead/scintillator sampling calorimeter", Osaka Masters Thesis, 4 Feb 1999.
8. H. Watanabe, "Measurement of Photon Detection Inefficiency in Total Absorption Calorimeters for the Measurement of $B(K_L^0 \to \pi^0\nu\bar{\nu})$", Saga University Masters Thesis, 1998.
9. H. Watanabe, "Reanalysis of photon detection inefficiencies for the KEK-CsI and 1mm-Pb/3mm-Scinti calorimeters", KEK-ES171 Internal Report (date unknown).

10. T. Matsumura, "Measurement of the detection inefficiency for photons of energies 90 to 1000 MeV", RCNP Masters Thesis, 4 Feb 1999.
11. K. Sakashita, "Measurement of the photon detection inefficiency due to photonuclear interactions", Osaka Masters Thesis, 24 Apr 2002.
12. D. Marlow, "Photo-Nuclear Absorption and the E787 Photon Veto", E787 Technical Note 31, (1984).
13. D. Marlow, "The Impact of E787 Mechanical Design on Photon Detection Efficiency", E787 Technical Note 83, (1985).
14. C. Woody, "Limiting Photon and π^0 Detection Efficiencies for Various Photon Veto Configurations", E787 Technical Note 116, (1986).
15. P. Meyers, "Measurement of the π^0 Inefficiency and an Upper limit on the Process $\pi^0 \to \nu\bar{\nu}$", E787 Technical Note 165, (1989).
16. P. Meyers, "Monte Carlo Studies of π^0 Inefficiency", E787 Technical Note 197, (1990).
17. A. Konaka, "A Monte Carlo study of holes in the photon detection", E787 Technical Note 247, (1992).
18. M. Kazumori, "A Study on Photon Detection Improvement for the $K^+ \to \pi^+\nu\bar{\nu}$ Experiment at BNL", University of Tokyo Masters Thesis (1997).
19. K. Manabe, "Bottom Up Study of $K_L \to \pi^0\nu\bar{\nu}$ experiment", Osaka Masters Thesis, 25 Mar 2000.
20. M.S. Atiya, et al., "A detector to search for $K^+ \to \pi^+\nu\bar{\nu}$", NIM **A 321** (1992) 129.